Indian Journal of Chemical Technology
Vol. 28, January 2021, pp. 36-46

A green tactic for inhibition of corrosion on mild steel in bore well water by aqueous extract of *Bauhinia Blakeana* leaves

K Geetha & R Udhayakumar*

Department of Chemistry, Anna University, BIT Campus, Tiruchirappalli 620 024, Tamilnadu, India.

E-mail: udhaya0123@gmail.com

Received 3 January 2020; 27 August 2020

The impact of an aqueous extract of *Bauhinia Blakeana* leaves (AEBBL) in controlling the corrosion of mild steel in bore well water medium has been demonstrated by mass loss method and electrochemical measurements. The extract is characterized by Fourier-Transform Infrared Spectroscopy (FTIR) and the active ingredients present in the AEBBL are identified by Gas Chromatography-Mass Spectrometry (GC-MS). The surface morphology is examined with the help of Scanning electron microscopy (SEM) and the surface roughness analysis is done by Atomic force microscopy (AFM). Weight loss method reveals that 8 $per\ cent\ v/v$ of the extract offers a maximum corrosion inhibition efficiency of 96.62%. Potentiodynamic polarization study (PDP) and Electrochemical impedance spectroscopy (EIS) are used to study the mechanistic aspects of corrosion inhibition. Both the double layer capacitance (C_{dl}) and corrosion current (I_{corr}) values decreases while the charge transfer resistance (R_{ct}) value increases with the increase in concentration of AEBBL. The potentiodynamic polarisation reveal that AEBBL acts as mixed type inhibitor with primarily cathodic effectiveness. SEM and AFM documented the development of shielding coating on the mild steel surface.

Keywords: AFM, *Bauhinia Blakeana*, Bore well water, EIS, GCMS, Mild steel

Corrosion is a universal occurrence and prevention of corrosion becomes one of the challenging phenomena in the modern world. When a reactive metal or alloy is exposed to environment, the gases and water present in air react gradually with the metal surface and form their corresponding oxides, carbonates, sulphates etc. This eating up of a metal by the environment is called as corrosion. The World Corrosion Organization estimates the global cost of corrosion to be about USD $2.5 trillion annually[1]. By adopting proper technology, about 25 to 30 percentage of this corrosion lost could be avoided. Corrosion prevention should not be considered as a financial issue, but also one of the health and safety issue to the environment[2]. Due to high strength, ease of fabrication and low cost, iron and steel are widely used in the steel frame buildings, machinery parts, cookware, pipelines, storage tanks for water, liquid chemicals and petroleum products, paints, water treatment plant, oil industries, biofuel, visually aesthetic metal gate, fencing etc.[3,4]. Mild steel is one of the grade of steel (low carbon steel - % C = 0.05% to 0.25%) and is typically used due to their low cost, excellent weldability, easy to cut and drill. But its corrosion resistance is very poor and easily subjected to corrosion if not properly maintained. In industries corrosion of carbon steel becoming a maddening problem and are triggered by various corrosive environment predominantly acids, sea water and saline formation water[5-7]. The inevitable corrosion of metals and alloys can be minimised by several techniques such as metallic coatings, cathodic protection method, sacrificial anodic method and adding corrosion inhibitors[8,9], among these the corrosion inhibitor is the much suitable technique because of their wide applicability in different sectors[10-12]. A corrosion inhibitor is a substance when added in a small concentration to an environment reduces the corrosion rate of a metal exposed to that environment[13]. Use of corrosion inhibitors is one of the finest ways to retard the corrosion rate of metals and alloys; even small concentrations of inhibitor retards the corrosion rate and possess good inhibition efficiency[14,15]. Organic compounds containing nitrogen, oxygen and sulphur atoms in their functional groups are generally used as corrosion inhibitors[16-18]. The use of these conventional inhibitors may be satisfactory towards corrosion prevention, but harmful to the environment. As far as several synthetic compounds have been verified as excellent corrosion

inhibitors, but majority of them have disadvantages like toxic nature, expensive, non-biodegradable[19]. Environmental problems should be of primary concern for the importance of protection and prevention of ecosystem. So, the corrosion inhibitors must be non-toxic, lower cost, renewable, biodegradable, environment friendly, convenient to handle, give less wastage, no tension regarding the disposal. Thus, in recent years attempts have been focused towards the development of eco-friendly green corrosion inhibitors such as plant extracts as a promising and gifted alternative source for corrosion inhibitors[20-31]. The active chemical constituents present in different parts of the plant majorly consists heteroatoms like nitrogen, oxygen, sulphur and multiple bonds which will adsorbed on the metal surface[32-37]. Hence, Plant products are rich sources of green corrosion inhibitors. In the past two decades, many research have been done on the corrosion inhibition of various metal and alloys by using various extracts of different parts of a plant like leaves, flowers, fruits, seeds, barks and roots[38-44]. Due to non-toxic and eco-friendly nature, the aqueous extract of plant materials are used as economic and green corrosion inhibitors. Literature survey reveals that so far no analysis has been done on the corrosion inhibitive efficiency of AEBBL. In this present study AEBBL was chosen for the inhibition of mild steel in bore well water. The presence of heteroatoms in AEBBL was identified by GC-MS. The corrosion inhibition efficiency was tested via weight loss method and Tafel polarization study. The protective deposition formed on the mild steel surface in the inhibitor system was proved by using surface analysis such as SEM and AFM. The formation of metal-inhibitor complex on the mild steel surface was confirmed by FTIR, UV-visible and Fluorescence spectrometer.

Experimental Section

Metal

The metal specimens taken for this study is mild steel and its elemental composition is Fe – 99.5%; C– 0.1020%; Si – 0.0720%; Mn – 0.1970%; P– 0.0280% and others –0.1010. The dimension of the metal specimen used for the weight loss method was 1.5 cm × 4 cm × 0.1 cm and for the electrochemical, SEM and AFM study was 1 cm × 1 cm × 0.1 cm. The metal specimens were polished with 1000, 1500, 2000 grades of emery sheet, washed with double distilled water and finally decreased with tricholoroethylene and used for the entire study.

Plant description

The scientific information of the *Bauhinia Blakeana*is given in the Table 1.

The *Bauhinia Blakeana* tree (Fig. 1) is the official floral emblem of Hong Kong and it is widely cultivated in tropical regions. It is sterile, which means it does not generally produce seeds or fruits and a hybrid between *Bauhiniavariegate* and *Bauhinia purpurea*.

Plant extract preparation

The leaves of *Bauhinia Blakeana* were collected from Tiruchirappalli District, Tamilnadu, India. The leaves were washed thoroughly with running tap water, dried under shade, powdered using mechanical grinder and sieved to get a fine powder. About 10 g of the powdered sample was soaked in 100 mL double distilled water in a stoppered container for a period of three days, first filtered using sieving mesh, further with WhatmanNo.1 paper and stored. This stock solution was added with bore well water to get different concentrations ($\% v/v$) of the corrosive medium.

Table 1 — Scientific classification of the plant

Kingdom	Plantae
Family	Fabaceae
Order	Fabales
Genus	Bauhinia
Species	B. × Blakeana
Botanical name	Bauhinia blakeana

Fig. 1 — *Bauhinia Blakeana* Tree

Medium

The present investigation was done in the bore well water which was taken from Tiruchirappalli, Tamilnadu, India. The water analysis of the water sample was done by the Department of Agriculture, Trichirappalli, Tamilnadu, India and is given in the Table 2.

Phytochemical analysis of AEBBL

The AEBBL was subjected to preliminary phytochemical screening for the confirmation of existence of phytochemicals by using standard methods mentioned by J. B. Harbrone (Table 3).

Gas chromatography-Mass spectrometry analysis of AEBBL

GC-MS is one of the advanced technique to identify the constituents of volatile matter, long chain and branched chain hydrocarbons, alcohols, acids, esters ect. GC-MS analysis was done on a SHIMADZU QP2020 system consisting of AOC-20i auto-sampler and gas chromatography interfaced to a mass spectrometer instrument. Interpretation of GC-MS spectrum was carried out using the database of National Institute Standard and Technology (NIST), having more than 62,000 patterns. The spectrum of unknown constituent was compared with spectrum of known constituent stored in NIST library. The name, molecular weight, formula and structure of the constituents present in AEBBL were ascertained. The concentrations of the individual constituents were determined through area and height normalization.

Weight loss method

Weight loss measurements were done using five digit balance model SARTORIUS, maximum weight of 220 g with accuracy. The cleaned, weighed mild steel specimens were immersed in bore well water without and with different concentration of AEBBL for 72 h using glass hooks. After the immersion period the metal specimen were washed with double distilled water, dried and then reweighed. The above procedure was repeated again and the average mass loss values were obtained. From the weight loss, the rate of corrosion and percentage of inhibition efficiency were calculated by using the following expressions.

$$\%I.E = \frac{W_o - W}{W_o} \times 100 \quad \ldots (1)$$

W_o – Weight loss in bare medium; W – Weight loss in inhibitor system

$$CR = \frac{87.6 \times W}{ATD} mpy \quad \ldots (2)$$

$w =$ Loss in weight (mg); $D =$Density (gcm^{-3}); $A =$ Surface area of the metal specimen (cm^2); $T =$ Time in hours (h)

$$\text{Surface coverage, } \theta = \frac{\%I.E}{100} \quad \ldots (3)$$

Electrochemical measurements

Electrochemical measurement was conducted in a CHI electrochemical work station, model 660A. It was equipped with automatic iR compensation facility. A three electrode cell assembly having a capacity of 100 ml was used. Mild steel (1 cm^2) was as working electrode, platinum as counter electrode and standard calomel electrode (SCE) as reference electrode. Salt bridge is used to connect the saturated calomel electrode with the test solution. Before each

Table 3 — Phytochemical screening of AEBBL

Phyto-constituents	Inference
Carbohydrates	+
Reducing sugar	-
Hexose sugar	+
Non-Reducing sugar	-
Proteins	+
Amino acids	-
Tyrosine	-
Steroids	+
Glycosides	+
Anthraquinone glycosides	-
Saponin glycosides	+
Cyanogenic glycosides	-
Alkaloids	+
Tannins	-
Phenolic compounds	-
Flavonoids	-
Terpenoids	+
Saponins	+

Table 2 — Report of water analysis of the bore well water

Parameters	Range	Parameters	Range	Parameters	Range
*p*H	7.39	Calcium	13.3 ppm	Residual Sodium Carbonate	-
Carbonate	0.4 ppm	Magnesium	8.7 ppm	Sodium Adsorption ratio	2.74
Bicarbonate	2.8 ppm	Sodium	9.07 ppm	Calcium -Magnesium ratio	0.65
Chloride	28.1ppm	Potassium	0.23 ppm	Sulphate	-

run, the working electrode was immersed in the test solution for 10 minutes to attain a steady state open circuit potential. All experimental studies were done at room temperature (27℃).

Potentiodynamic polarization study

The Tafel polarisation curves were determined by scanning the electrode potential to $\pm 300\, mV$ with respect to the E_{corr} at a scan rate of $1\, mV^{-1}$. The corrosion parameters such as corrosion potential (E_{corr}) and corrosion current (I_{corr}) were calculated. The inhibition efficiency percentage (% I.E) and degree of surface coverage (θ) was evaluated from the measured I_{corr} values using the following relations.

$$\%\, I.E\ = \frac{i_{corr} - i_{corr}(inhibitor)}{i_{corr}} \times 100 \qquad \ldots(4)$$

Electrochemical impedance spectroscopy analysis

The formation of the protective film on the metal surface, resistance and capacitance at the interface, adsorption mechanism of corrosion inhibition can be clearly understood by EIS technique. EIS measurements were carried out in a frequency range of 100000 to 0.1 Hz at amplitude of 10 mV peak-to-peak. The measure of electron transfer across the metal surface is known as $R_{ct.}$ The maximum frequency at the imaginary component of the impedance is f_{max}. The C_{dl} was calculated at this f_{max} by using the following equation:

$$C_{dl}\ = \frac{1}{2\pi f_{max} R_{ct}} \qquad \ldots (5)$$

Fourier-transform infrared spectroscopy analysis

FTIR analysis was used to evaluate the plant extract and the inhibitive layer formed on the metal surface for identifying the functional group. The metal specimens were hanged in the medium with AEBBL by means of hooks. After 72 h the metals were taken out, washed with double distilled water and dried. Then the inhibitive film developed on the metal surface was scratched off and taken for the FTIR spectral study. The analysis was carried out in Perkin Elmer FTIR spectrometer with the wavenumber range of 4000 to 400 cm^{-1} . The background material used is KBr.

UV- Visible spectroscopy analysis

UV visible spectroscopy or Electronic spectroscopy is an important tool in analytical chemistry which involves the promotion of electrons present in the valence shell from the ground state to higher energy level or excited state when subjected to light. The analysis was done by using Perkin-Elmer, Lambda 35 UV-Visible spectroscopy with a range of 190 nm to 1100nm which is a PC controlled single beam scanning spectrophotometer. The possibility of interaction of iron with the inhibitor molecules was observed by analysing the AEBBL and AEBBL extract containing ferrous ion.

Fluorescence spectroscopy analysis

Fluorescence spectroscopy is a type of electromagnetic spectroscopy which analyses the fluorescence from a sample. It involves a beam of light, usually ultraviolet light, excites the electron in certain molecules and cause them to emit light. The fluorescence spectra of the AEBBL extract containing ferrous ion and the film formed on the metal surface in the inhibitor system were recorded using Perkin Elmer, LS 45 spectrofluoro meter with the range of 200 to 900 nm.

Scanning electron microscopy analysis

SEM is a type of electron microscope that provides a pictorial representation of the metal surface. It images a sample by scanning with a beam of electrons in a raster scan pattern. The metal specimens were immersed in the medium with the presence and absence of AEBBL for 72 h, removed, washed with double distilled water and then dried well. To examine the nature of the protective film formed on the metal surface and the corrosion inhibitive efficiency, the SEM micrographs of the polished metal surface, corroded metal in bare medium and the metal immersed in the inhibitor system were examined by using ZEISS instrument.

Atomic force microscopy analysis

AFM is becoming a powerful technique to investigate the roughness data of the surface and is very significant to confirm the inhibition efficiency of the extract on the metals. It provides two-dimensional and three-dimensional image by imaging the force of the uneven contacts of the tip with the metal surface. The metal specimens were immersed in the medium with the presence and absence of AEBBL for 72 h, removed, washed with double distilled water and then dried well. The instrument used was BT 02218 – Nanosurf. It is

helpful to gather roughness statistics such as average roughness (R_a), root mean square roughness (R_q) and maximum peak to valley height (P-V) in nano scales. From the above mentioned data, the extent of corrosion inhibition can be evaluated.

Results and Discussion

Phytochemical analysis of AEBBL

The result obtained on preliminary screening for phytochemicals of AEBBL is given in the Table 3.

The above table illustrates the presence of phytochemicals like Proteins, Steroids, Glycosides, Alkaloids, Terpenoids and Saponins with the functional group containing oxygen, nitrogen and sulphur. The presence of these active constituents is responsible for corrosion inhibitive action.

GC-MS analysis of AEBBL

The GC-MS chromatogram of AEBBL showed twenty two peaks which indicate the presence of twenty two active chemical constituent in it. The Table 4 represented the various active principles with their retention time (RT), molecular formula, molecular weight and percentage area. Among these twenty two constituents, two constituents namely Dodecanoic acid, 1,2,3-propanetriyl ester and Dodecanoyl chloride are the predominant constituents. On examining the structures of the above listed compounds, it is evident that the phytochemicals present in AEBBL are rich in heteroatoms, π electrons, aromatic rings which are responsible for the inhibition process by facilitating the charge transfer from the inhibitor's molecule to the charged metal surface. Structure of some phytochemicals present in the AEBBL is given in Fig. 2.

Weight loss method

Inhibition efficiency (% IE), corrosion rate (CR) and surface coverage (θ) values calculated from the weight loss method for mild steel with the absence and presence of different concentrations of AEBBL at room temperature are summarised in Table 5. From the table, it is evident that as the concentration of inhibitor increases, inhibition efficiency increases, rate of corrosion decrease and surface coverage increases. The maximum inhibition efficiency of 96.62% was attained for mild steel when immersed in 8 per cent v/v of extract concentration.That is, the

Table 4 — Chemical constituents identified in the GCMS analysis of AEBBL

Peak	RT	Area %	Compound name	Formula	Mol. wt.
1	23.695	1.05	Methanesulfonamide, N-methyl-N-(6-oxo-1-cyclohexen-1-yl)	$C_8H_{13}NO_3S$	203
2	26.03	0.8	Methyl 6-hydroxycaproate	$C_7H_{14}O_3$	146
3	28.695	0.73	Ethanone, 1-(methylenecyclopropyl)	C_6H_8O	96
4	34.04	0.84	2-(3-Fluoro-Phenylmethanesulfonyl)-3H-imidazo[4,5-B]pyridine	$C_{13}H_{10}FN_3O_2S$	291
5	34.105	2.8	1H-Indole-3-ethanamine	$C_{10}H_{12}N_2$	160
6	34.907	0.91	2-(2-Ethyl-1-hydroxyhexyl)cyclohexanol	$C_{14}H_{28}O_2$	228
7	35.26	0.19	4-Iodohistidine, methyl ester	$C_7H_{10}IN_3O_2$	295
8	35.771	1.88	Phenanthrene, 9-dodecyltetradecahydro	$C_{26}H_{48}$	360
9	36.595	0.82	1-Triethylsilyloxyheptadecane	$C_{23}H_{50}OSi$	370
10	36.676	1.77	1H-Indole-3-ethanamine	$C_{10}H_{12}N_2$	160
11	37.34	4.69	Tetracosanoic acid, methyl ester	$C_{25}H_{50}O_2$	382
12	37.493	27.95	Dodecanoic acid, 1,2,3-propanetriyl ester	$C_{39}H_{74}O_6$	638
13	37.63	23.58	Dodecanoyl chloride	$C_{12}H_{23}ClO$	218
14	37.703	17.03	Dodecanoic acid, 1,2,3-propanetriyl ester	$C_{39}H_{74}O_6$	638
15	37.875	3.72	1H-1,2,3-Triazole-5-methanol, 1-amino-4-phenyl	$C_9H_{10}N_4O$	190
16	37.955	1.08	3-(Dideuteromethoxymethoxy)-2,3-dimethyl-1-undecene	$C_{15}H_{28}D_2O_2$	244
17	38.06	0.64	1-Tripropylsilyloxytridec-2-yne	$C_{22}H_{44}OSi$	352
18	38.159	1.2	4H-1-Benzopyran-4-one, 2-(3,4-dihydroxyphenyl)-6,8-di-.beta.-D-glucopyranosyl-5,7-dihydroxy	$C_{27}H_{30}O_{16}$	610
19	38.255	0.77	Benzene, 1,1'-(2-methylene-1,3-propanediyl)bis	$C_{16}H_{16}$	208
20	38.398	2.83	2-Pentanone, 4-cyclohexylidene-3,3-diethyl	$C_{15}H_{26}O$	222
21	39.689	3.84	(4AR,9AS,9BS)-4A,6,6,9A-Tetramethyl-trans-perhydroindano [2,1-C]pyran	$C_{16}H_{28}O$	236
22	39.76	0.85	Cyanamide, N-allyl-N-[2-(2-hydroxy-2-methylpropyl)-3,3-dimethylcyclopropyl] methyl	$C_{14}H_{24}N_2O$	236

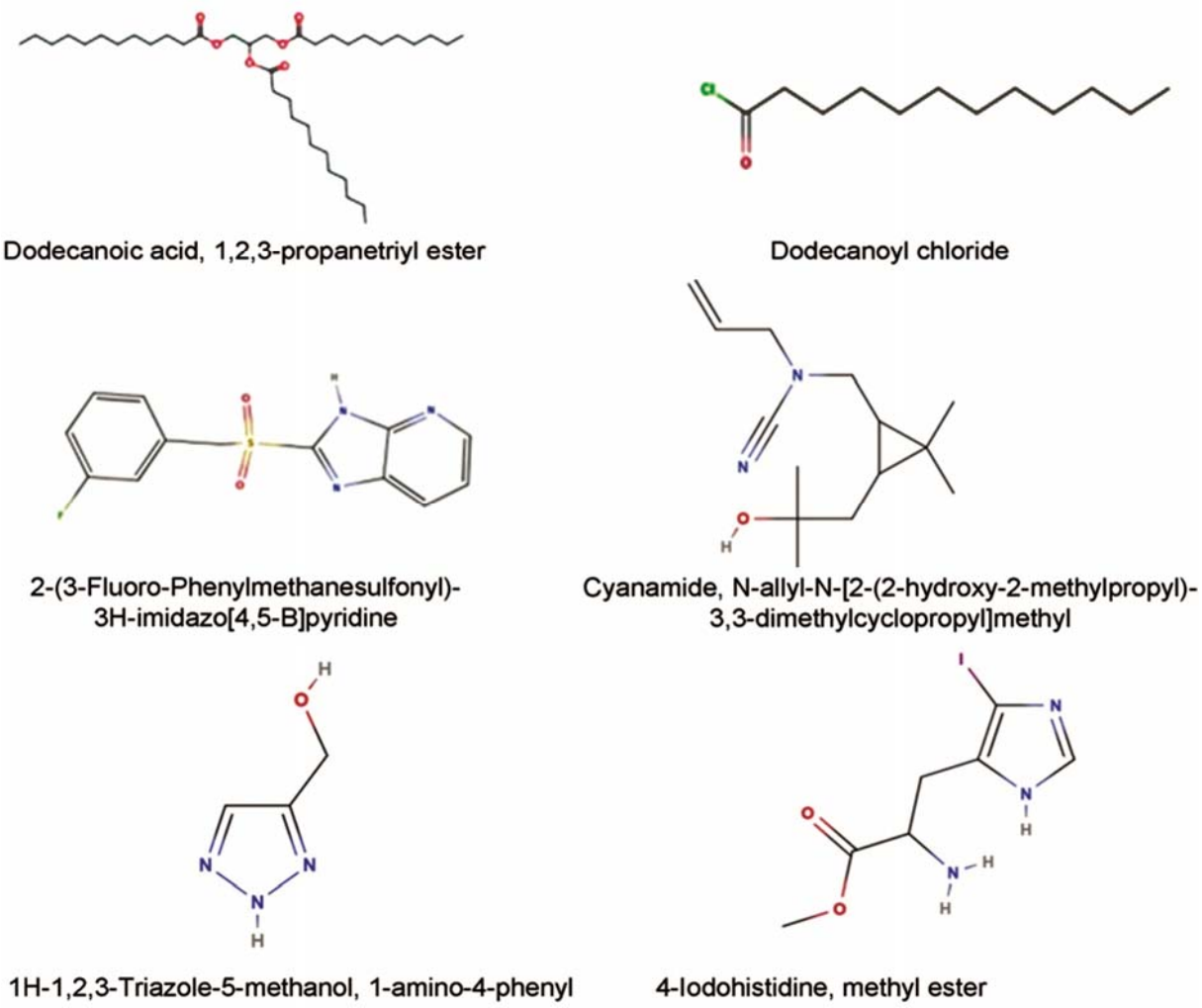

Fig. 2 — Structure of some of the phytochemicals present in the AEBBL

Table 5 — Inhibition efficiency of AEBBL on mild steel corrosion at different concentrations from weight loss method

S. No	Conc. of inhibitor (%)	Wt. Loss (g)	% IE	CR (mpy)	θ
1	Blank	0.01241	-	172.36	-
2	2	0.00079	93.63	10.97	0.9363
3	4	0.00065	94.76	9.03	0.9476
4	6	0.00061	95.08	8.47	0.9508
5	8	0.00042	96.62	5.83	0.9662
6	10	0.00059	95.24	8.19	0.9524

oxidation of mild steel is decreased by the coverage of active molecules from the inhibitor on the metal surface.

Potentiodynamic polarization method

The polarization behaviour of mild steel in the absence and presence of various concentrations of AEBBL is given in Fig. 3. It was reported that, an inhibitor can be classified as cathodic or anodic type,

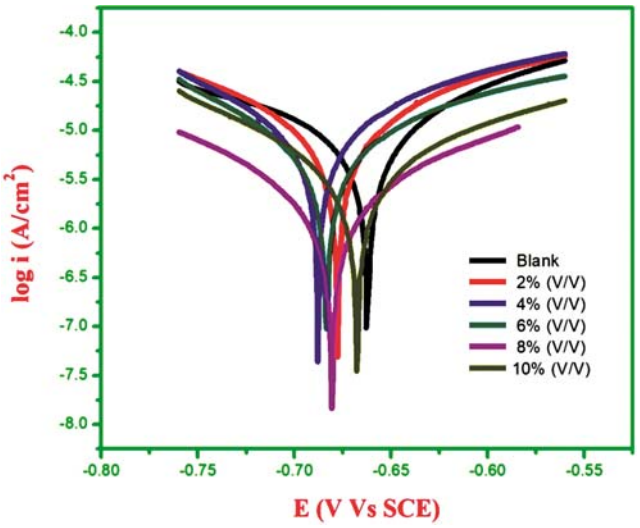

Fig. 3 — Tafel plot of mild steel in bore well water medium in the absence and presence of different concentrations of the AEBBL

if the shift in corrosion potential is more than ±85 mV with respect to the corrosion potential in the absence of inhibitor[45]. From the Table 6, it is inferred that as the inhibitor concentration increases, the corrosion potential (E_{corr}) value shifts to more negative direction but the difference in corrosion potential is less than ±85 mV, behaves as an mixed type inhibitor with primarily cathodic effectiveness. On addition of AEBBL to bore well water, the corrosion current (i_{corr}) are found to decrease. The inhibition efficiency and surface coverage are increases when compared to blank. 8 $per\ cent\ v/v$ AEBBL offers a maximum inhibition efficiency of 93.55%for mild steel. The above inferences indicate that the corrosion rate of the mild steel reduced through the formation of adsorbed protective film on the metal surface.

Electrochemical impedance spectroscopy analysis

Figure 4 shows that Nyquist plot of mild steel in bore well water in the absence and presence of different concentration of AEBBL extracts. Table 7 inferred that as the concentration of the inhibitor increases, the diameter of the capacitive loops also increases which reveals the good shielding of metal surface from the corrosion medium by higher coverage of inhibitor molecules on mild steel. R_{ct} increases with increase in concentration of the extract which is inversely proportional to corrosion rate. Development of protective deposit diminishes double layer capacitance (C_{dl}) by boosting charge transfer resistance.

Table 6 — Tafel polarization parameters of mild steel in bore well water with different concentrations of AEBBL

S. No.	Conc. of inhibitor (%)	E_{corr} (V)	$I_{corr}(\mu A)$	% IE	θ
1	Blank	-0.662	40.287	-	-
2	2	-0.678	26.024	35.4	0.3540
3	4	-0.688	20.664	48.7	0.4870
4	6	-0.684	13.931	65.42	0.6542
5	8	-0.682	2.598	93.55	0.9355
6	10	-0.668	7.874	80.45	0.8045

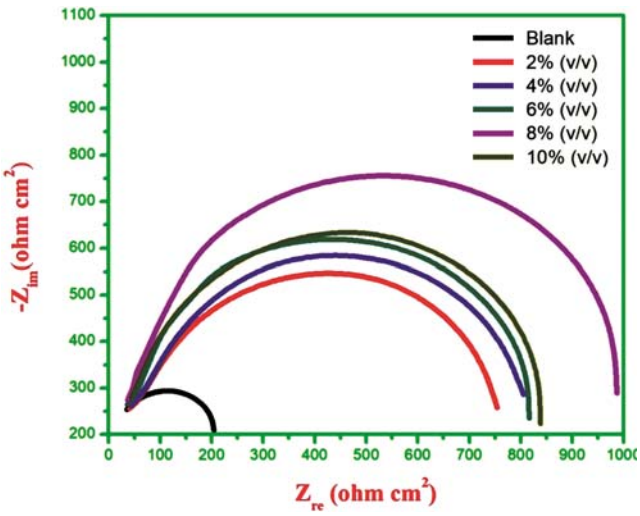

Fig. 4 — Nyquist plot of mild steel in bore well water medium in the absence and presence of different concentrations of the AEBBL

FTIR analysis

FT-IR is used to identify the functional groups present in the AEBBL. The active constituents in the extract contribute towards corrosion inhibition through the heteroatoms present in its functional groups. The absorption bands for FT-IR spectral study of AEBBL and Surface film formed are shown in Table 8. The shift in the absorption band reveals the interaction of the inhibitor with the metal surface. The FT-IR spectra of AEBBL and corrosion product formed in the inhibitor system are given in Figs 5a and 5b. Some new bands were formed in the film coating due to the formation of new bonds on the metal surface which appreciably provide inhibition of corrosion of the mild steel[46]. These results lead to the

Table 7 — EI Sparameters of mild steel in bore well water with different concentrations of AEBBL

S. No.	Conc. of inhibitor (%)	R_{ct} $(ohm\ cm^2)$	C_{dl} $(\mu F\ cm^{-2})$	% IE
1	Blank	169.18	3.20	-
2	2	714.66	0.40	76.33
3	4	762.17	0.35	77.80
4	6	780.60	0.32	78.33
5	8	950.06	0.22	82.19
6	10	796.05	0.30	78.75

Table 8 — FT-IR absorption bands for AEBBL and the film formed on the metal surface

Assignment	Peak (cm^{-1})	
	AEBBL	Surface Film
O−H stretching (alcohol) / N−H stretching (1^o amine)	3411.73	3432.83
O−H stretching (carboxylic acid)	2921.14	2926.26
C−H stretching (alkane)	2852.03	2856.17
C=O stretching	1650.20	1644.06
S=O stretching	1318.04	1337.89
C−H stretching ($-CH_2X$)	1260.60	1171.20
C−N stretching	1074.20	1075.31
N−H stretching (amines)	894.51	868.28
C−Cl stretching	618.91	607.77
Fe_2O_3	----	697.73

conclusion that the protective layer formed on the metal surface consists of metal-inhibitor complex as a result of coordination of functional group of natural products in extract with Fe^{2+} formed on the metal surface.

UV- Visible analysis

UV-Visible spectroscopy offers a strong support for the formation of metal-complex. The peaks in the UV-Visible spectrum may arise due to the $\pi - \pi^*$ and $n - \pi^*$ electronic transitions[47]. The UV-Visible absorption spectrum of AEBBL and AEBBL with Fe^{2+} ($FeSO_4 . 7H_2O$). Peak shifts from 274.9 to 546.7nm. This shift in the peak positions and change in the absorbance values confirm the formation of metal-inhibitor complex on the metal surface.

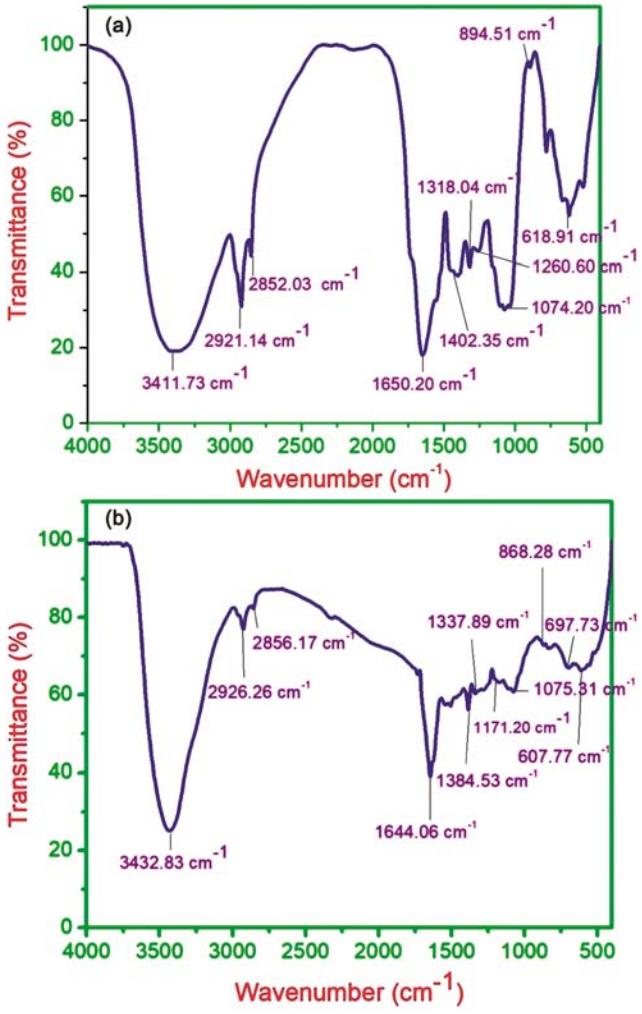

Fig. 5 — (a) FT-IR spectra of AEBBL & (b) FT-IR spectra of surface film formed on the metal surface in the presence of inhibitor

Fluorescence analysis

The fluorescence spectrum of AEBBL with Fe^{2+} ($FeSO_4 . 7H_2O$) is shown in Fig. 6a. Peak appears at 399.57nm, 551.751 nm and 634.08nm. The fluorescence spectrum of the inhibitive film developed on the mild steel surface in the inhibitor system is shown in Fig. 6b. Peak appears at 399.07nm, 551.10nm and 701.18 nm.The peaks in the surface film spectra match with the peaks in the AEBBL. Thus, it is confirmed that the surface film consists of Fe^{2+} - inhibitor complex.

SEM analysis

Figure 7a illustrates that the polished surface was smooth and free from pits. Figure 7b of mild steel exposed to bore well water in the absence of extract

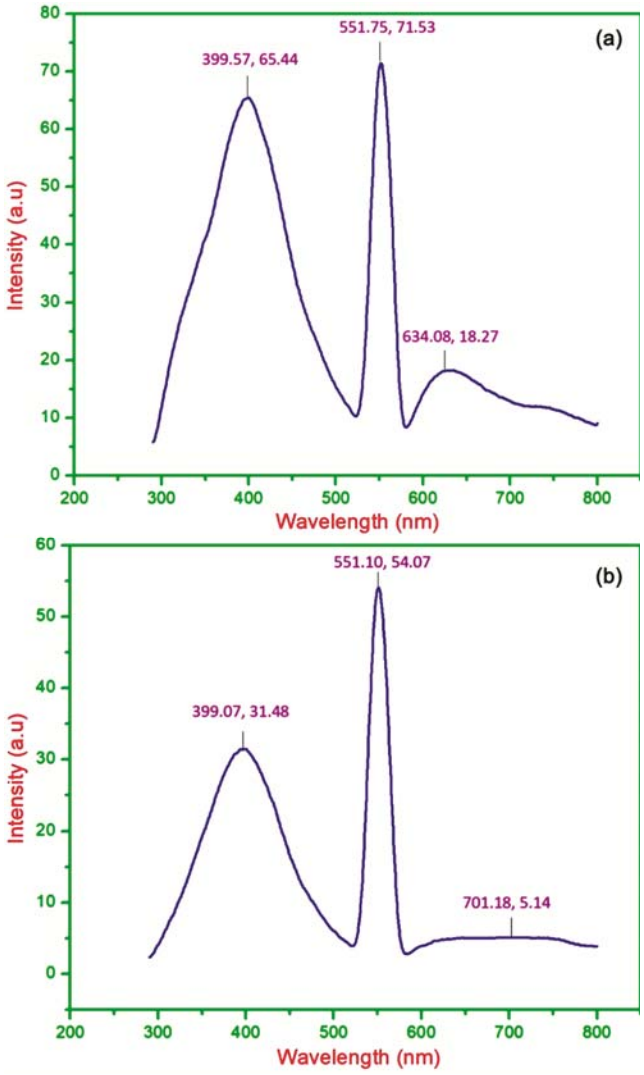

Fig. 6 — (a) Fluorescence spectra of AEBBL with Fe^{2+} (b) Fluorescence spectra of surface film formed on the metal surface in the presence of inhibitor

was highly cracked and rich in pits owing to metal dissolution. However, in Figure 7c of mild steel in optimum concentration of AEBBL, the pits are reduced and comparatively a smooth surface is obtained. The reason for this structure is blocking of active sites on the metal surface by adsorption of inhibitor molecules. Moreover, a thin protective coating was formed at the metal surface and consequently enhances the corrosion resistance[48]. The increase in surface coverage results in the accumulation of insoluble metal – inhibitor complex on the metal surface which retards the corrosion of mild steel.

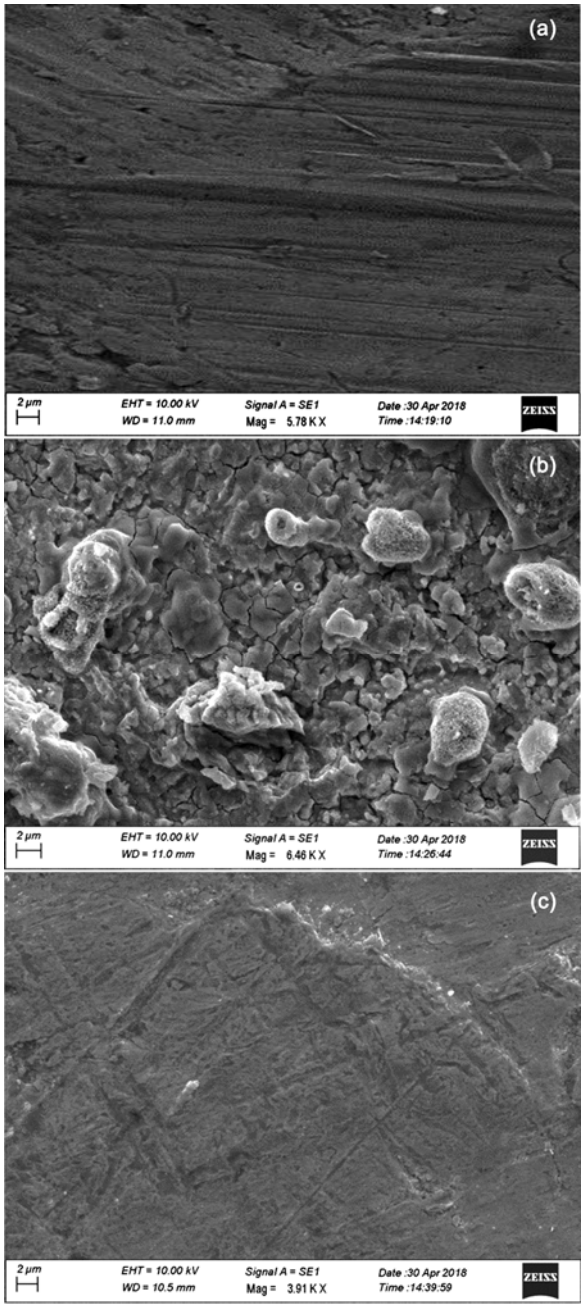

Fig. 7 — (a) Polished mild steel, (b) Corroded mid steel and (c) Protected mild steel with AEBBL

AFM analysis

The topography of polished mild steel surface, corroded mild steel surface in the absence of extract and the protected mild steel surface with the AEBBL are shown in Figs 8a, 8b and 8c respectively.

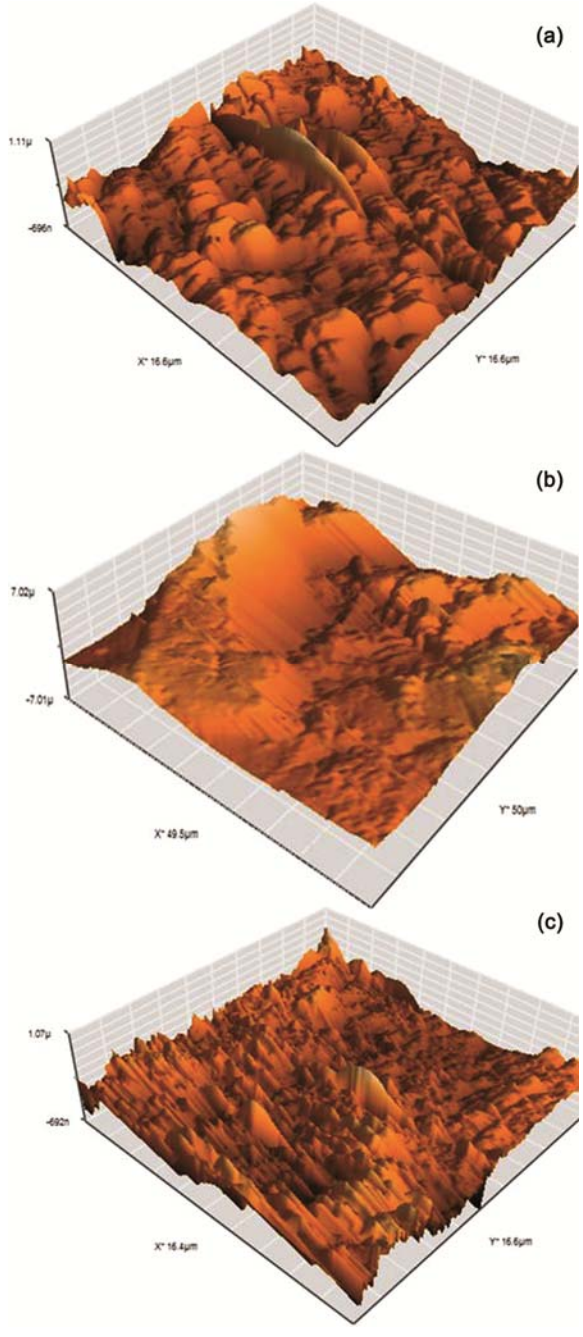

Fig. 8 — (a) Polished mild steel, (b) Corroded metal & (c) Mild steel with AEBBL

The AFM parameters - average roughness (R_a), root mean square roughness (R_q) and maximum peak to valley height (P-V) are listed in the Table 9. The average surface roughness for the polished mild steel is 75.687 nm. The average roughness for the corroded mild steel is increased to 1283.2 nm due to the dissolution of mild steel in the bore well water. While for the inhibited mild steel in the presence of AEBBL, the value of average roughness is 134.58 nm lower than that of the corroded mild steel. This decrease in the average roughness is due to the adsorption of phytoconstituents from the inhibitor on the mild steel surface[49]. The topography and roughness data give a clear indication of formation of inhibitive layer on the mild steel surface.

Corrosion mitigation mechanism

The essentialneed for inhibition is a metal having low energy vacant electron orbital and a molecule with heteroatoms containing a lone pair of electrons or aromatic/heterocyclic rings or conjugated bonds. The inhibition of mild steel in the studied environment can be described by the adsorption of the constituents of AEBBL on the mild/solution interface. The adsorption may occurs through the (a) electrostatic interaction between the charged inhibitor molecules and the charged metal surface (b) co-ordination of the unshared electron pairs on the heteroatoms of the inhibitor molecules to the vacant d-orbitals of metal surface atoms (c) donor- acceptor interaction of π bonds (conjugated bonds) in the inhibitor molecules with metal[50,51]. In aqueous solutions, the AEBBL may exist either as neutral molecules or as protonated AEBBL. AEBBL might be protonated in the solution as follows:

$$AEBBL + xH^+ \rightarrow [AEBBLH_x]^{x+} \quad \ldots (6)$$

By means of electrostatic attraction between $OH^-$and protonated AEBBL, the AEBBL constituents can be attached to the mild steel surface.

Table 9 — AFM roughness parameters for polished, corroded and protected mild steel

S. No	System	R_a (nm)	R_q (nm)	R_y (nm)
1	Polished mild Steel	75.687	99.397	597.52
2	Corroded mild steel in bore well water	1283.2	1423.9	5208.7
3	Inhibited mild steel in bore well water with 8 ml of AEBBL	134.58	153.92	636.27

$$Inhibitor_{(solution)} + xH_2O_{(adsorbed)} \rightarrow Inhibitor_{(adsorbed)} + xH_2O_{(solution)} \quad \ldots (7)$$

$$M \rightarrow M^{2+} + 2e^- \quad \ldots (8)$$

$$M^{2+} + AEBBL \rightarrow [M - AEBBL]_{(adsorbed)}{}^{2+} \quad \ldots (9)$$

The neutral AEBBL molecules can be adsorbed on the mild steel by displacement of one or more water molecules which are initially adsorbed at the metal surface. The AEBBL molecules can also be adsorbed on the metal surface through donor-acceptor interactions between π – electrons of inhibitor molecules and vacant d-orbital of metal. This adsorption process blocks the active centres on the metal surface and suppresses the corrosion rate. The extent of inhibition depends upon the adsorption power which is influenced by number of active sites on the metal surface, chemical structure and molecular size of the inhibitor molecules, the mode of interaction between the inhibitor and metal, charge distribution of metal and inhibitor, nature of the metal-inhibitor complex formed on the surface[52]. The relative solubility of the metal-inhibitor complex decides the further mitigation or acceleration of metal dissolution. The slight decrease in the inhibition efficiency after a certain critical concentration of the extract (8ml) can be expounded on the basis of competitive adsorption[53]. At the critical concentration, the mild steel surface is completely covered with the AEBBL molecules. Above the critical concentration, the un-adsorbed inhibitor molecules compete with those already adsorbed on the metal surface to replace them, thereby producing bare places on the metal surface or holes in the protective film, thus the water can attack the metal surface, corrosion takes place and reduces the corrosion resistance.

Conclusion

- The characterisation of the extract by phytochemical screening and GC-MS suggests AEBBL possess anti-corrosive property on mild steel owing to the presence of heteroatoms contained phytoconstituents.
- FTIR results proved the presence of functional groups containing heteroatoms which is responsible for the formation of protective layer on metal/ medium interface.
- AEBBL shows maximum inhibition efficiency at8 $per\ cent\ v/v$ of extract concentration for

weight loss study, potentiodynamic polarisation measurement and electrochemical impedance spectroscopy analysis.

- PDP measurements inferred that AEBBL behaves as a mixed type inhibitor with cathodic predominance.
- The SEM and AFM analyses showed that the inhibition of mild steel occurred by the development of inhibitive film on the metal surface through adsorption of the constituents of AEBBL.
- Inhibition efficiency **v**alues resulted from various corrosion study techniques are in reasonable agreement which leads to conclude that AEBBL being a natural and environment benign product can be employed as active green corrosion inhibitor for mild steel in bore well water medium.

References

1 Gupta R K, Malviya M, Verma C & Quarishi M, *Mater Chem Phys*, 198 (2017) 360.
2 Khamis E & Al Andis N, *Mater Wiss Werks Tech*, 9 (2002) 550.
3 Abd El-Lateef H M, Abu-Dief A M & Mohamed M A A, *J Mol Struct*, 1130 (2017)522.
4 Zhu Y, Free M L & Yi G, *Corros Sci*, 98 (2015) 417.
5 El-Taib Heakal F, Attia S K, Rizk S A, Abou Essa M A & Elkholy A E, *J Mol Struct*, 1147 (2017) 714.
6 Karthik G & Sundaravadivelu M, *Egypt J Pet*, 25 (2016) 183.
7 Fekry A M & Mohamed R R, *Electrochim Acta*, 55 (2010) 1933.
8 Nagarajan S, Mohana M & Sudhagar P, Raman V, Tishimura T, Kim S, Kang Y S & Rajendran N, *ACS Appl Mater Interface*, 4 (2012) 5134.
9 Peabody A W, Bianchetti R & Ronald L. Bianchetti, *Control of Pipeline Corrosion* (National Association of Corrosion Engineers) 1967.
10 Hamdani N El, Fdil R, Tourabi M, Jama C & Bentiss F, *Appl Surf Sci,* 357 (2015) 1294.
11 Sin H LY, Rahim A A, Gan C Y, Saad B, Salleh M I & Umeda M, *Measurement*, 109 (2017) 334.
12 Liu Zhang L, Yan X, Lu X, Gao Y & Zhao C, *Corros Sci,* 93 (2015) 293.
13 Roberge P R, *Handbook of Corrosion Engineering* (Mc Graw Hill) 2000.
14 Raja P B & Sethuraman M G, *MaterLett*, 62 (2008) 113.
15 EL-Etre A Y, *Corros Sci*, 40 (1998) 1845.
16 Ansari K R, Quraishi M A & Singh A, *Corros Sci*, 79 (2014) 5.
17 Nam N D, Somers A, Mathesh M, Seter M, Hinton B, Forsyth M & Tan M Y J, *Corros Sci*, 80 (2014) 128.
18 Abboud Y, Abourriche A, Saffaj T, Berrada M, Charrouf M & Bennamaraetal A, *Mater Chem Phys*, 105 (2007) 1.
19 Chaubey N, Savita, Singh V K & Quraishi M A, *J Assoc Arab Univ Basic Appl Sci*, 22 (2017) 38.
20 Zucchi F & Omar I, *Surf Technol*, 24 (1985) 391.
21 Abdel-Gaber A M, Khamis E, Abo-El Dahab H & Adeel S, *Mater Chem Phys*, 109 (2008) 297.
22 Avwiri G O & Igho F O, *Mater Lett*, 57 (2003) 3705.
23 Abdel-GaberA M, Abd-El-Nabey B A & Saadawy M, *Mater Corros*, 63 (2012) 161.
24 Mehdipour M, Ramezanzadeh B & Arman S Y, *J Ind Eng Chem*, 21 (2015) 318.
25 Yaro S, Khadom A & Wael K, *Alexandria Eng J*, 52 (2013) 129.
26 Weina Su, Tian Yimei & Peng S, *Appl Surf Sci*, 315 (2014) 95.
27 Obi-Egbedi N O, Obot I B & Umoren S A, *Arabian J Chem*, 5 (2010) 361.
28 Shweta S, Dixit R D & Sahu T R, *Int J Tradit Knowl*, 4 (2005) 392.
29 Singh A K, Mohapatra S & Paniet B, *J Ind Eng Chem*, 33 (2016) 288.
30 Yadav D K, Chauhan D S, Ahamad I & Quireshi M A, *RSC Adv*, 3 (2013) 632.
31 Lashgari M & Malek A M, *ElectrochimActa*, 55 (2010) 5253.
32 Emad E El-Katori & Saedah Al-Mhyawi, *Green Chem Lett Rev*, 12 (2019) 31.
33 Alaneme K K, Daramola Y S, Olusegun S J & Afolabi A S, *Int J Electrochem Sci*, 10 (2015) 3553.
34 Okewale A O & Olaitan A, *Int J Mater Chem*, 7 (2017) 5.
35 Deyab M A, Osman M M, Elkholy A E & El-Taib Heakal F, *RSC Adv*, 7 (2017) 45241.
36 Helen L Y S, Rahim A A, Saad B, Saleh M I & Bothi Raja P, *Int J Electrochem Sci*, 9 (2014) 830.
37 Verma C, Quraishi M A, Eno Ebenso E & Bahadur I, *J Bio Tribo Corros*, 4 (2018) 33.
38 Jamiu Kolawole Odusote, Olorunfemi Michae, Ajayi Raheem & AboloreYahya, *J Electrochem Sci Eng*, 4 (2014) 67.
39 Ghadah M Al-Senani & Mashael Alshabanat, *Int J Electrochem Sci*, 13 (2018) 3777.
40 Rocha J C, *Corros Sci*, 52 (2010) 2341.
41 Deyab M A, *Desalination*, 384 (2016) 60.
42 El Bribri A, Tabyaoui M, Tabyaoui B, El Attari H & Bentiss F, *Mater Chem Phys*, 141 (2013) 240.
43 Umoren S A, Solomon M M, Obot I B & Sulieman R K, *J Ind Eng Chem*, 76 (2019)91.
44 Al-Senani M & Mashael Alshabanat, *Int JElectrochem Sci*, 13 (2018) 3777.
45 Riggs J O L, *Theoretical aspect of corrosion inhibitors and inhibition*, First edition, (Houston: National Association of Corrosion Engineering) 1973.
46 Paul Ocheje Ameh, Alhaji Modu Kolo, Aminu Ahmed & Isaac Kayode Ajanaku, *J Ind Environ Chem*, 1 (2017) 15.
47 Ambrishsingh, Yuanhua Lin, Eno E. Ebenso, Wanying Liu & Bo Huang, *Int J Electrochem Sci*, 9 (2014) 5993.
48 Prabhu R A, Venkatesha T V, Shanbhag A V & Kulkarni G M, *Corros Sci*, 50 (2008) 3356.
49 Akhil Saxena, Dwarika Prasad & Rajesh Haldhar, *Int J Electrochem Sci*, 12 (2017) 8793.
50 Ostovari A, Hoseinieh S M, Peikari M, Shadizadeh S R & Hashemi S J, *Corros Sci*, 51 (2009) 1935.
51 Antonijevic M M & Petrovic M B, *Int J Electrochem Sci*, 3 (2008) 1.
52 Fouda A S, Moussa M N, Taha F I & Elneanaa A I, *Corros Sci*, 26 (1986) 719.
53 Zhao J M, Duan H B & Jiang R J, *Corros Sci*, 91 (2015) 108.